euspen's 20th International Conference & Exhibition, Geneva, CH, June 2020
www.euspen.eu

# Design and hard machining of a high performance ceramic impeller

E. Uhlmann[1, 2], J. Polte[1], S. Koprowski[1], J. Kochan[1], T. Borsoi Klein[1]

[1]*Fraunhofer Institute for Production Systems and Design Technology IPK, Pascalstr. 8-9, 10587 Berlin, Germany*
[2]*Institute for Machine Tools and Factory Management IWF, Technische Universität Berlin, Pascalstr. 8-9, 10587 Berlin, Germany*

*tiago.borsoi.klein@ipk.fraunhofer.de*

**Abstract**
The constant development and improvement of mechanical and chemical properties of high performance ceramics allows the expansion of its actual applications. In comparison to metal materials, the use of novel high performance components can offer numerous advantages. In turbomachinery, a full ceramic impeller can fulfil the requirements of efficiency and high turbine inlet temperatures combined with lower cooling requirements, reduced combustion emissions and fuel consumption. This is feasible not only thanks to the properties of the ceramics, but also by the interaction of this with simulation, design optimization, manufacturing processes and a high quality finishing by hard machining. However, the machining of brittle material components with complex geometries remains a challenge in terms of resultant surface characteristics, tribological properties, geometric accuracy and process costs. In this scenario, 5-axis grinding with mounted points and innovative strategies provide new possibilities for the manufacturing of these complexes components. The current work aims at a practice-oriented design and the following hard machining of a hot isostatically pressed silicon nitride (HIPSN) impeller with complex geometry and high requirements, gathering low geometrical deviations, reduced brittle fractures and roughness at the ground part. To achieve these objectives, different machining strategies and parameters are tested and correlated with the resulting quality of the component. Simulation techniques are also shown to ensure optimum operating conditions for the ceramic component.

5-axis grinding, kinematics, sculptured surfaces, Silicon Nitride

## 1. Introduction

The demand for high efficient turbomachinery systems such as aircraft engines, stationary gas turbines, as well as turbochargers for engines is constantly growing due to the increasing need for energy and mobility worldwide [1]. Moreover, the concern to reduce the environmental impact of power generation, e.g. emissions of NOx and CO, and the commercial pressure for continuous improvement in engine performance and fuel efficiency have driven the development of new materials with increasing temperature resistance and performance capability [2-4]. In this context, high performance ceramics can offer many advantages in comparison to nickel-based superalloys [5-12]. However, besides market growth, the challenges faced by industry in order to produce and machine such materials are also growing.

Regarding the difficulties of using high performance ceramics as structural material in critical components of turbine components, two are described in the current work. The first is the redesign of an actual impeller needed to support the high stresses at high temperature while using materials with relative low critical fracture toughness $K_{Ic}$. The second is the machining of such components to achieve high geometric accuracy and obtain a crack free surface.

This work describes the development of a design and hard machining strategies of a HIPSN turbine impeller in order to achieve a component able to raise the turbine inlet temperature and therefore its efficiency. Critical geometries of the current impeller are pointed out and changes are suggested to enable the material exchange. Within complex geometries, the tool orientation during hard machining of such component plays a major role on the resultant surface characteristics. The current work is focused on the 5-axis grinding using spherical mounted points, in with thin and large surfaces with complex geometries are complained.

## 2. Experimental Setup

### *2.1. General Information*

The original metal material of the impeller was replaced by HIPSN developed in the Fraunhofer Institute for Ceramic Technologies and Systems IKTS. The material replacement, (metal to ceramic) requires changes in the component's design, originally from one microturbine with a rating of P = 30 kW. The design adjustment was supported by CFD simulation and a structural heat transfer simulation. The final CAD model for a ceramic impeller is shown in Fig. 1. An material oversize of approximately a = 0.2 mm was left during the injection to guarantee the final dimensions of the part through hard machining.

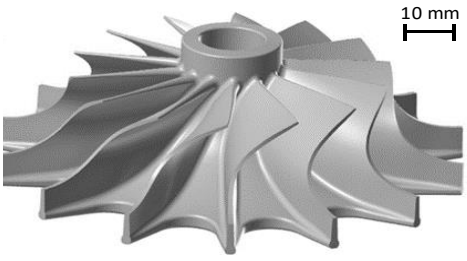


**Figure 1.** Optimized CAD model of a ceramic impeller

The hard machining followed four steps: definition of the grinding strategies and kinematics, generation of a CAM code, roughing and finishing processes.

### *2.2. Grinding machine and process parameters*

Grinding experiments were conducted at the FRAUNHOFER IPK facilities on a 5-axis machining center RXP 600 DSH UHP, manufactured by the company RÖDERS GMBH, Soltau, Germany. The high-precision machine is equipped with an automatic tool changer, an integrated acoustic emission (AE) system, an integrated tactile workpiece measurement system as well as an internal dressing unit. The cooling lubricant employed was the grinding oil Rotex Spezial V 1734-2, manufactured by MKU CHEMIE GROUP, Rödermark, Germany. For the technological investigation, single layer grinding tools with diamond abrasive grains were used. Table 1 shows the grinding and sharpening parameters for the investigations.

**Table 1 Grinding and sharpening parameters for the investigations**

| | | |
|---|---|---|
| *Grinding parameters* | | |
| Peripheral wheel speed $v_s$ | 21 | m/s |
| Depth of cut $a_e$ | variable | mm |
| Feed rate $v_f$ | variable | mm/min |
| Cooland flow rate $Q_{KSS}$ | 3 x 6 | l/min |
| *Sharpening parameters* | | |
| Feed rate $v_{fSb}$ | 200 | mm/min |
| Depth of cut $a_{eSb}$ | 2 | mm |
| Height of sharpening block $h_{Sb}$ | 6 | mm |
| *Grinding tool* | | |
| Tool diameter $d_s$ | 8 | mm |
| Tool length $l$ | 60 | mm |
| Grain type | D126/D64 | |
| Bond type | Electroplated | |
| Abrasive grain concentration | G10/G20 | |
| *Workpiece* | | |
| Material | $Si_3N_4$ | |

The roughness was measured with a optic measurement system InfiniteFocus manufactured by the company BRUKER ALICONA, GRAZ, Austria, using a lateral resolution of $l_r$ = 1 µm and vertical resolution of $v_r$ = 0.075 µm. A first order filter was applied to generate the primary profile from the measured profile.

## 3. Results

### *3.1. Generation of a turbomachinery impeller design adapted to ceramic properties*

The turbine impeller, loaded by a maximal rotation of n = 96.000 rpm, is to be substituted by a monolithic ceramic impeller. In contrast to metallic materials, ceramics exhibit about six times lower thermal expansion ratio and a considerably lower tensile strength. Thus, it is necessary to create on the one hand a ceramic-suitable impeller design and on the other hand a construction concept to assemble metal and ceramic components.

The computer aided design (CAD) process requires the detailed knowledge of the loads acting to the turbomachinery system during assembly and in operation. Additionally to the mechanical clamping load and the centrifugal forces, the thermal loads resulting from the hot gas flow are considered.

The solid temperature distribution is the result of a "multi-physical" process: the exhaust gas flow induces a heat flux whose sign and magnitude is depending on the wall temperature of the solid. In turn, the wall temperature is determined by the heat flux from the gas flow and other thermal boundary conditions. Thus, a cosimulation between a turbomachinery CFD simulation (FINE/Turbo) and a structural heat transfer simulation (ABAQUS) has been performed until thermal equilibrium is reached. The code coupling tool (MpCCI CouplingEnvironment) was used for the data exchange management at run-time. With these mechanical and thermal loads, first feasibility studies were realized and a ceramic design was developed. As shown in Fig. 2, mainly the chamfers have been replaced by radii and the press fit between the ceramic impeller and the metallic axle was removed. Moreover, the inner bore hole is shaped conically. Furthermore, conical metallic washers were introduced which allow a centering of the impeller while the different thermal expansions are compensated by radial slipping.

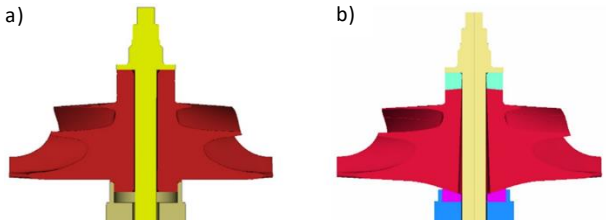


**Figure 2.** (a) Original metalic impeller with tie rod and air bearing and (b) basic design features

The frictional connection between the parts is realized with a clamping concept. Due to the different thermal expansions of the components materials the pretension force for the assembling had to be adapted. The materials are: Inconel (axle), ceramic (impeller) and aluminum (compressor). Therefore it was necessary to choose an initial pretension load, which, after reduction by heating, is high enough to transfer the resulting torque from the fluid to the axle.

The final step of the ceramic-suitable design process was an algorithmic optimization of the impeller geometry starting from the developed basic design. A multi-target optimization based on response surfaces was performed in order to create a design with reduced mechanical stresses. Since the basic shape of the flow channel is not to be changed, the blade thickness, the scallop radii, the blade root radius, the conical angles of the bore and the washers and the height of the washers served as parameters. The optimization work-flow was set up using the software modeFRONTIER, where several automation scripts (ANSA, metaPost) are applied.

In this way, it was possible to generate multiple designs, which meet the high requirements concerning the maximal tensile stress (< 340 MPa) and the manufacturing conditions. For the final design was achieved using performance (FINE/Turbo) and vibration (MpCCI FSIMapper, ABAQUS) simulations.

### *3.2. Grinding strategies*

The strategies and kinematics to grind a micro-turbine impeller are limited by the size and detail level of the features to be ground, access of the tool to the features, among others. According to JOSHI AND CHANG [13], features are regions of a part having some manufacturing significance in the context of machining. Examples of such features are hole, slop, pocket, etc. The current work is focused at the machining of complex features. Therefore, features formed by the rotation or translation of a straight line in the workpiece coordinate system (WCS), such as the features shown in Fig. 3, are not discussed in the current work. Moreover, these features are preferentially ground using cylindrical tools.

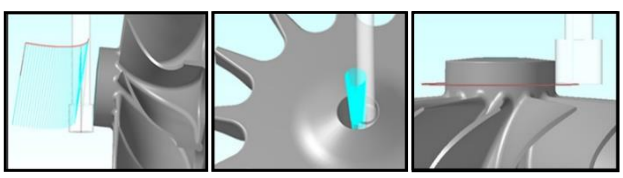

**Figure 3.** Examples of features to be ground [15]

One of the key parameter regarding 5-axis grinding is the stepover $f_s$. This parameter represent the distance between two parallel tool paths while grinding a surface and result in the theoretical roughness Rth while using spherical mounted points (also named scallop height). For the features shown in Fig. 4, the surfaces are machined using a single path of the tool. Therefore, stepover $f_s$ have no significant influence on the process and on the ground surface.

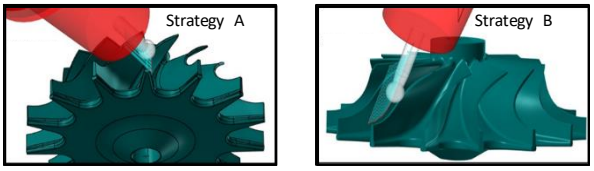


**Figure 4.** CAM simulation for the strategies A and B [15]

Figure 4 shows the strategies A and B described in the current work. The kinematics used in the strategy A is based on the tool orientation coordinated by tilt $\beta_{fN}$ and lead $\beta_f$ angles. These were selected to result in a tool inclination of $\alpha$ = 30° and a structure angle of $\alpha_s$ = 45° . For the strategy B, the tool was positioned tilted 30° to the impeller axis, resulting in the variation of the structure angle $\alpha_s$ within the ground surface. For both strategies, the cutting speed in the center of the groove was $v_c$ = 10.5 m/s, the feed rate was $v_f$ = 200 mm/min and the depth of cut was $a_e$ = 0.020 mm. The strategies C, D, E and F are based on the feature shown at the Fig. 5. This feature is a wide surface and need to be machined with parallel passes of the tool (using the parameter stepover $f_s$). The grinding strategy defines the tool path. Examples of such strategies are zig-zag, one way, contour parallel to the border and spiral. At the current work, this feature was ground with roughing (strategy C) and finishing parameters (strategies D, E and F) using an spiral strategy centred on the impeller axis.

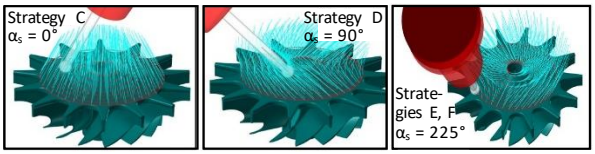


**Figure 5.** CAM simulation for the strategies C, D, E and F [15]

For the roughing process, strategy C, the surface was ground using stepover $f_s$ = 0.5 mm and depth of cut $a_e$ = 0.02 mm. To increase the area of the tool in contact with the workpiece after a complete tool rotation and the chip flow efficiency during the roughing, a tilt angle $\beta_{fN}$ = 30° was applied, resulting in a structure angle of $\alpha_s$ = 0°.

**Table 2. Complementary table of the grinding parameters for the grinding of the ceramic impeller**

| **Strategy** | **A** | **B** | **C** | |
|---|---|---|---|---|
| Process | Finishing | Finishing | Roughing | |
| Structure angle as | 45.00 | variable | 0.00 | degree |
| Inclination angle γ | 30.00 | variable | 30.00 | degree |
| Lead angle βf | 20.70 | variable | 0.00 | degree |
| Tilt angle βfN | -22.21 | variable | 30.00 | degree |
| Depth of cut ae | 0.02 | 0.02 | 0.02 | mm |
| Stepover fs | - | - | 0.50 | mm |
| Cutting speed vc | 10.50 | 10.50 | 10.50 | m/s |
| Feed rate vf | 200.00 | 200.00 | 1000.00 | mm/min |
| Tool diameter ds | 8.00 | 8.00 | 8.00 | mm |
| Grain size D | 126.00 | 126.00 | 126.00 | µm |

| Strategy | D | E | F | |
|---|---|---|---|---|
| Process | Finishing | Finishing | Finishing | |
| Structure angle $\alpha_s$ | 90.00 | 225.00 | 225.00 | degree |
| Inclination angle γ | 30.00 | 30.00 | 30.00 | degree |
| Lead angle $\beta_f$ | 30.00 | -20.70 | -20.70 | degree |
| Tilt angle $\beta_{fN}$ | 0.00 | 22.21 | 22.21 | degree |
| Depth of cut $a_e$ | 0.01 | 0.01 | 0.01 | mm |
| Stepover $f_s$ | 0.10 | 0.10 | 0.10 | mm |
| Cutting speed $v_c$ | 10.50 | 10.50 | 10.50 | m/s |
| Feed rate $v_f$ | 1000.00 | 1000.00 | 1000.00 | mm/min |
| Tool diameter $d_s$ | 8.00 | 8.00 | 8.00 | mm |
| Grain size D | 126.00 | 126.00 | 64.00 | µm |

### *3.3. Analysis of the ground surface*

The analysis of different features frequently demand different methods. Therefore, the ground surfaces in the current work were analysed in two parts: the ground surfaces without (strategies A and B) and with the influence of the stepover fs (strategies C, D, E and F). Fig. 6 shows the optic measurement of thin surfaces ground without stepover $f_s$ . For the machining of such features, the borders play a major role in the analysis of the machining quality.

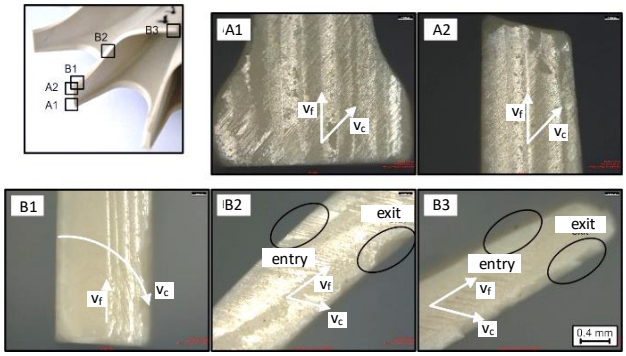


**Figure 6.** Optic measurement of the turbine impeller: strategies A and B [15]

Grinding with a structure angle $\alpha_s$ = 45° tend to reduce the surface roughness due to the scratches tilted in relation to the feed direction, even in thin walls. The measurement of the strategy A shows no significant brittle fractures in the entrance nor the exit of the abrasive grains along the surface border. Some brittle fractures were observed over the surface, however, repeated in the feed direction. This behaviour results from a protruding grain on the tool, which increases the material removal in a limited zone. The optic measurement of the surface ground with strategy B reveals a high amount of brittle fractures along the surface border. These are concentrated in the exit of the abrasive grains over the surface. No significant fractures were observed along the borders on the entrance side of the surface. The difference between the exit border in the strategies A and B shown the influence of the vibration during grinding process, in which strategy B (specifically B3 in Fig. 6) represents the most susceptible part of the impeller to vibrate. Figure 7 shows the values of Sa, Sz, Spk, Sk and Svk for the strategies C, D, E and F, measured with an optic measurement device. For the grinding of a large surface, roughness parameters are initially employed (strategy C) to achieve a high material removal rate. The gain in the material removal rate reflect in the surface quality, resulting in the highest values of Sa, Sz, Spk and Sk.

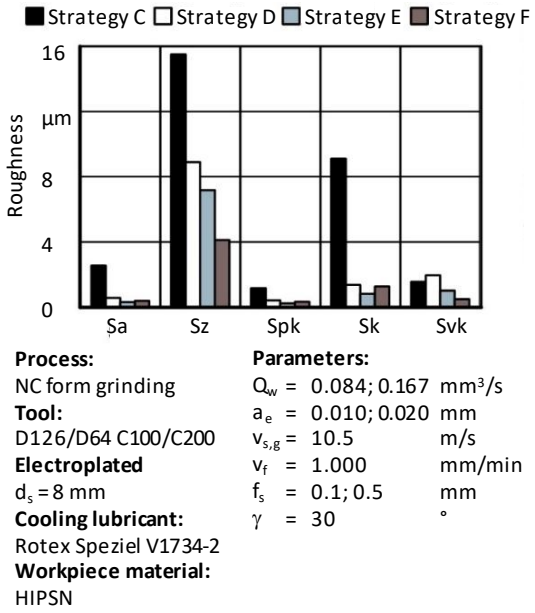


**Figure 7.** Surface parameters for the strategies C, D, E and F [15]

A reduction on the stepover from $f_s$ = 0.5 mm to $f_s$ = 0.1 mm reduces the value of the theoretical roughness from Rth = 7.8 µm to 0.3 µm. Low values of stepover $f_s$ and depth of cut $a_e$ result in a high geometrical accuracy on the final workpiece (strategies D, E and F). Regarding to the kinematic parameters, reductions of 43 % of Sa, 19 % of Sz, 48 % of Spk, 40 % of Sk and 48 % of Svk were observed while changing the structure angle from $\alpha_s$ = 90° (strategy D) to $\alpha_s$ = 225° (strategy E). The strategy E is the strategy with the optimized grinding and kinematic parameters. Not only the lowest geometric deviation are observed but also the lowest surface roughness. However, brittle fractures were randomly observed over the ground surface for the strategies C, D and E. The strategy F possess the same grinding and kinematic parameters than the strategy E, with exception of the grinding tool. The size of the abrasive grains for the strategy F is D = 64 µm (126 µm for the previous strategies). This alteration changed not only the surface roughness (see Fig. 7), but also the material removal mechanisms. No significant brittle fracture was observed on the surface ground for the strategy F.

Grinding with spherical mounted points allows high flexibility regarding the kinematic to be employed. According to UHLMANN [14], the scratches on the workpiece for grinding with structure angle $\alpha_s$ = 90° or $\alpha_s$ = 270° are perpendicular to the feed direction F. The joint action of the abrasive grains over the tool surface changes the real depth of cut $a_e$ to the grains located in different positions over the tool. The reduction on the grain size result in this case in higher amount of grains over the tool surface.

## 4. Summary and conclusions

High performance ceramics can be used as alternative material in the turbomachinery, bringing advantages such as higher efficiency and reduction of the combustion emissions. The current work investigates the design and the hard machining of a HIPSN turbine impeller. To achieve a functional HIPSN turbine impeller, a redesign in its geometries is required. A ceramic-suitable design gather a proper co-simulation between turbomachinery CFD simulation and structural heat transfer simulation. Furthermore, the optimized machining of such component can be achieved using proper grinding parameters, kinematics and tools. The following conclusions can be drawn from the current work:

- The grinding kinematic, defined by the tool orientation during process, represent an important factor on the final characteristics of the ground part.
- The tilt and lead angles can be used on 5-axis grinding to create structures on the ground surface, hence reducing its roughness.
- High values of stepover $f_s$ results in high removal material rate $Q_w$, however, resulting in high values of roughness on the ground surface.
- By reducing the abrasive grain size and increasing its concentration, the number of cutting edges increases. Thus, the material removal rate $Q_w$ for one cutting edge reduces, resulting in a reduction of the amount of brittle fractures on the ground surface.

## References


[1] F. Klocke, A. Klink, D. Veselovac, D. K. Aspinwall, S. L. Soo, M. Schmidt, J. Schilp, G. Levy, and J.-P. Kruth: Turbomachinery component manufacture by application of electrochemical, electro-physical and photonic processes, CIRP Annals - Manufacturing Technology, vol. 63, no. 2, pp. 703 – 726, 2014.

[2] R. E. Hester and R. M. Harrison: Environmental Impact of Power Generation, vol. 11. Cambridge: Royal Society of Chemistry, 1999.

[3] H. Fecht and D. Furrer: Processing of nickel-base superalloys for turbine engine disc applications, Advanced Engineering Materials, vol. 2, no. 12, pp. 777 – 787, 2000.

[4] K. König-Urban: Additive fertigung von nickelbasis-superlegierungen mittels laserstrahlschmelzen am beispiel von diamalloy 400 ns, 2015.

[5] J. G. Lee and I. B. Cutler: High-performance ceramics, Journal of the Korean Ceramic Society, vol. 14, no. 1, pp. 33 – 49, 1977.

[6] G. W. Meetham: The Development of Gas Turbine Materials. Dordrecht: Springer Netherlands, 1981.

[7] J. R. Price, O. Jimenez, L. Faulder, B. Edwards, and V. Oarthasarathy: Ceramic stationary gas turbine development program: ASME International Gas Turbine and Aeroengine Congress and Exhibition. New York, N.Y.: ASME, 1998.

[8] J. R. Nicholls: Advances in coating design for high-performance gas turbines, MRS Bulletin, vol. 28, no. 09, pp. 659 – 670, 2003.

[9] E. Uhlmann, M. Bilz, J. Baumgarten, and T. Borsoi Klein: Innovative high-performance ceramics challenge for the life cycle engineering of turbo-machinery, Procedia CIRP, vol. 29, pp. 323 – 328,2015.

[10] A. Julian-Jankowiak, R. Valle, and M. Parlier: Potential of innovative ceramics for turbine applications, Materials at High Temperatures, vol. 33, no. 4 – 5, pp. 578 – 585, 2016.

[11] F. Watanabe, T. Nakamura, and K.-i. Shinohara: The Application of Ceramic Matrix Composite to Low Pressure Turbine Blade: ASME Turbo Expo 2016: Turbomachinery Technical Conference and Exposition. Seoul, South Korea, June 13 – 17. 2016.

[12] N. Kochrad, N. Courtois, M. Charette, B. Picard, A. Landry-Blais, D. Rancourt, J.-S. Plante, and M. Picard: System-Level Performance of Microtur- bines with an Inside-Out Ceramic Turbine: Journal of Engineering for Gas Turbines and Power. 2017.

[13] S. Joshi and T. C. Chang: Graph-based heuristics for recognition of machined features from a 3d solid model, Computer-Aided Design, vol. 20, no. 2, pp. 58 – 66, 1988.

[14] S. Koprowski, E. Uhlmann, and W. Weingaertner: Influence of tilt and lead angles on 5-axis grinding with spherical mounted points, Production Engineering, vol. 12, pp. 449 – 455, feb 2018.

[15] S. Koprowski: Grinding of high performance materials with spherical mounted points. Berlin TU Diss. ISBN 978 – 3 – 8396 – 1311 – 5. 2017.